

## Gallium diffusion in zinc oxide via the paired dopant-vacancy mechanism

T. N. Sky, K. M. Johansen, H. N. Riise, B. G. Svensson, and L. Vines

Citation: *Journal of Applied Physics* **123**, 055701 (2018); doi: 10.1063/1.5000123

View online: <https://doi.org/10.1063/1.5000123>

View Table of Contents: <http://aip.scitation.org/toc/jap/123/5>

Published by the [American Institute of Physics](#)

---

### Articles you may be interested in

[Iron and intrinsic deep level states in Ga<sub>2</sub>O<sub>3</sub>](#)

*Applied Physics Letters* **112**, 042104 (2018); 10.1063/1.5020134

[Guest Editorial: The dawn of gallium oxide microelectronics](#)

*Applied Physics Letters* **112**, 060401 (2018); 10.1063/1.5017845

[Rethinking the theoretical description of photoluminescence in compound semiconductors](#)

*Journal of Applied Physics* **123**, 055703 (2018); 10.1063/1.5008810

[Tuning the optical bandgap in multi-cation compound transparent conducting-oxides: The examples of In<sub>2</sub>ZnO<sub>4</sub> and In<sub>4</sub>Sn<sub>3</sub>O<sub>12</sub>](#)

*Journal of Applied Physics* **123**, 055704 (2018); 10.1063/1.5018056

[Effects of Ni doping and native point defects on magnetism of ZnO first-principles study](#)

*Journal of Applied Physics* **123**, 055106 (2018); 10.1063/1.5022780

[Enhanced ultraviolet photo-response in Dy doped ZnO thin film](#)

*Journal of Applied Physics* **123**, 054502 (2018); 10.1063/1.5015959

---

**AIP** | Journal of Applied Physics

SPECIAL TOPICS



# Gallium diffusion in zinc oxide via the paired dopant-vacancy mechanism

T. N. Sky,<sup>a)</sup> K. M. Johansen, H. N. Riise, B. G. Svensson, and L. Vines

*Department of Physics/Center for Materials Science and Nanotechnology, University of Oslo, P.O. Box 1048, Blindern, N-0316 Oslo, Norway*

(Received 14 August 2017; accepted 19 January 2018; published online 2 February 2018)

Isochronal and isothermal diffusion experiments of gallium (Ga) in zinc oxide (ZnO) have been performed in the temperature range of 900–1050 °C. The samples used consisted of a sputter-deposited and highly Ga-doped ZnO film at the surface of a single-crystal bulk material. We use a novel reaction diffusion (RD) approach to demonstrate that the diffusion behavior of Ga in ZnO is consistent with zinc vacancy ( $V_{Zn}$ ) mediation via the formation and dissociation of  $Ga_{Zn}V_{Zn}$  complexes. In the RD modeling, experimental diffusion data are fitted utilizing recent density-functional-theory estimates of the  $V_{Zn}$  formation energy and the binding energy of  $Ga_{Zn}V_{Zn}$ . From the RD modeling, a migration energy of 2.3 eV is deduced for  $Ga_{Zn}V_{Zn}$ , and a total/effective activation energy of 3.0 eV is obtained for the Ga diffusion. Furthermore, and for comparison, employing the so-called Fair model, a total/effective activation energy of 2.7 eV is obtained for the Ga diffusion, reasonably close to the total value extracted from the RD-modeling. *Published by AIP Publishing.*

<https://doi.org/10.1063/1.5000123>

## I. INTRODUCTION

Transparent and semiconducting zinc oxide (ZnO) has been extensively investigated over the past decades due to its desired and potential use in optoelectronic devices. Although the notorious n-type-only behavior of ZnO has impeded this realization, highly conductive n-type ZnO films used as a transparent conductive oxide (TCO) layer have been realized via doping by aluminium (Al) or gallium (Ga).<sup>1–3</sup> Controlling the dopant concentration and spatial distribution is essential for a vast range of applications and relies on an understanding of the diffusion process. For Al, both early studies and more recent ones, as well as density-functional-theory (DFT), report an activation energy for the diffusion in the range 2.6–2.7 eV.<sup>4,6</sup> For Ga, on the other hand, early work reported a pre-exponential factor and an activation energy of  $10^4 \text{ cm}^2 \text{ s}^{-1}$  and 3.75 eV,<sup>4</sup> respectively. More recent results indicated corresponding values of  $10^{-6} \text{ cm}^2 \text{ s}^{-1}$  and 1.47 eV,<sup>7</sup> while first-principles calculations estimated the activation energy to be 2.45 eV for Ga.<sup>6</sup> Hence, a significant discrepancy exists in the literature. Moreover, it has been shown that self-compensation occurs in Al and Ga doped ZnO,<sup>5,8</sup> thereby limiting its conductivity and applicability as TCO. For Al doping, the self-compensation is explained by the formation of zinc vacancies ( $V_{Zn}$ ) and a complex between  $V_{Zn}$  and substitutional Al at the zinc sub-lattice ( $Al_{Zn}$ ).<sup>5,9</sup> Further, the latter complex has been shown to be the main vehicle for Al diffusion.<sup>5</sup> The diffusion of an impurity atom and a vacancy as a paired complex was alluded in 1969 by Hu,<sup>10</sup> where it was proposed that the presence of Coulombic attraction between a charged vacancy and an oppositely charged dopant may tend to keep the vacancy in the vicinity of the dopant.

In this work, we combine experimental diffusion data and DFT data in a reaction diffusion (RD) model to show

that the diffusion of Ga in monocrystalline ZnO is vacancy mediated via the formation and dissociation of a  $Ga_{Zn}V_{Zn}$  complex. Moreover, quantitative estimates for the defect-dopant interplay are obtained due to the kinetics characteristics of the RD model used in the simulations.

## II. EXPERIMENT

A thin film of Ga-doped ZnO ( $2 \times 10^{21} \text{ cm}^{-3}$ ) was deposited onto hydrothermally grown single crystalline (0001-oriented) bulk ZnO samples (Tokyo Denpa) with a bulk resistivity of 1310  $\Omega \text{ cm}$ . The deposition was performed in a Semicore magnetron sputtering system using a 99.95% pure Ga-doped ZnO target ( $Zn_{0.9}Ga_{0.1}O$ ), resulting in a 1.6  $\mu\text{m}$  thick Ga-doped ZnO film. After the deposition, a laser-cut was made at the backside of the sample followed by cleavage into several small samples with a typical size of  $5 \times 5 \text{ mm}^2$ . One sample was sequentially heat treated for 30 min from 900 °C up to 1050 °C in stages of 50 °C to realize in-diffusion of Ga into the bulk material. In addition, a series of isothermal heat treatments for durations in the range of 20 min up to 5 h were performed on three different samples at 950, 1000, or 1050 °C. A Cameca IMS7f Secondary Ion Mass Spectrometer (SIMS) equipped with an  $O_2$  primary ion beam source was used to measure the concentration vs. depth profiles of Ga. Using a secondary ion field aperture, the circular gated region was 33  $\mu\text{m}$  diameter, ensuring a detected region only at the center of the 150  $\mu\text{m}^2$  sputtered crater bottom. Absolute concentration values of Ga were obtained by measuring a Ga ion implanted reference sample, ensuring less than  $\pm 10\%$  error in accuracy. Due to the highly Ga-doped ZnO deposited film and a dynamic range of typically 5 orders of magnitude for the SIMS analysis, the residual Ga-concentration in the as-grown ZnO was determined prior to the thin-film deposition and was found to be  $\sim 2 \times 10^{15} \text{ cm}^{-3}$ . For depth calibration, the sputtered crater

<sup>a)</sup>t.n.sky@fys.uio.no

depths were measured by a Dektak 8 stylus profilometer and a constant erosion rate was assumed.

### III. RESULTS AND DISCUSSION

Figure 1 shows the Ga concentration vs depth profiles for the sample heat treated sequentially for 30 min from 900 °C to 1050 °C. The characteristic box-like diffusion profiles, below the 1.6 μm thick deposited film, are similar to those observed in Al-diffused samples<sup>5</sup> and increase both in concentration and depth as a function of temperature. The large difference of more than one order of magnitude between the Ga concentration in the deposited film and in the bulk, which endures during the heat treatments, implies that a semi-infinite source condition is a valid assumption. However, a simple model assuming free diffusion from the semi-infinite source, giving solutions in the form of a complementary error function, fails to predict the abrupt diffusion front in Fig. 1, cf. also a similar conclusion for Al diffusion in ZnO.<sup>5</sup>

#### A. RD-model

In order to explain the diffusion of Ga and to gain physical insight into the defect reactions involved, we will primarily consider a RD type model,<sup>5,11–13</sup> combined with recent DFT calculations of Ga in ZnO.<sup>6</sup> The model is based on Fickian diffusion and adds a non-linear reaction term; for a theoretical outline of the RD model, see Refs. 5 and 11. In accordance with the work of Stiauf *et al.*,<sup>6</sup> we further presume that  $V_{Zn}^{-2}$  is the only mediating defect and take the dopant-vacancy complex to be the only vehicle for dopant migration, with a reaction according to



where  $Ga_{Zn}^{+}$  is regarded as immobile.

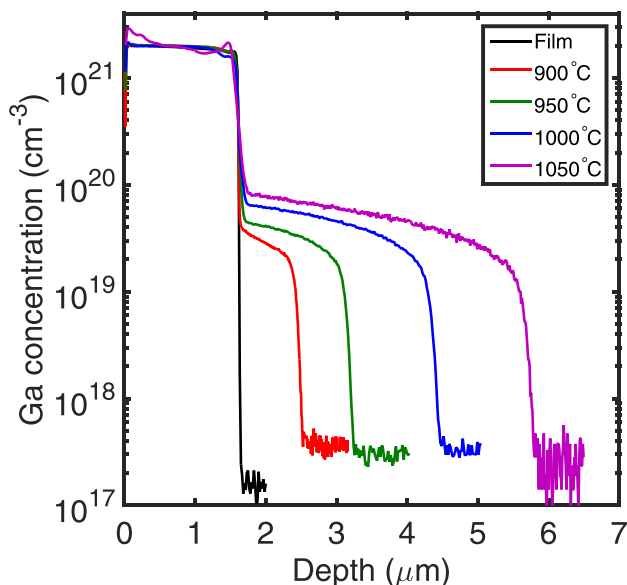


FIG. 1. Isochronal Ga diffusion profiles of the sample heat treated sequentially for 30 min from 900 °C to 1050 °C.

Here, it should also be emphasized that the deposited film of highly Ga-doped ZnO at the bulk crystal surface is considered as a source of  $(Ga_{Zn}V_{Zn})^{-}$  complexes, and not of  $Ga_{Zn}^{+}$ , in our RD-modeling. That is, already formed  $(Ga_{Zn}V_{Zn})^{-}$  complexes are injected into the bulk and their flux is treated as a boundary condition in the simulations. This assumption is corroborated by several theoretical and experimental results in the literature for the two analogous cases of Ga- and Al-doped ZnO.<sup>5,8,9,14,15</sup> Calculations based on DFT predict a significantly lower formation energy of  $(Ga_{Zn}V_{Zn})^{-}$  and  $(Al_{Zn}V_{Zn})^{-}$  complexes than that of isolated  $V_{Zn}^{-2}$  and  $Ga_{Zn}^{+}$  and  $V_{Zn}^{-2}$  and  $Al_{Zn}^{+}$ , respectively, in highly n-type samples under O-rich ambient conditions corresponding to those in the present experiments.<sup>5,14,15</sup> This prediction is supported by electron paramagnetic resonance (EPR) spectroscopy measurements revealing not only the atomic configuration of the  $(Al_{Zn}V_{Zn})^{-}$  complex but also that it prevails over  $V_{Zn}$  and  $Al_{Zn}$  by several orders of magnitude in MeV electron-irradiated samples with an Al concentration in the mid  $10^{17} \text{ cm}^{-3}$  range.<sup>9</sup> Furthermore, employing synchrotron X-ray absorption measurements and DFT, T-Thienprasert *et al.*<sup>15</sup> evidenced that the  $(Al_{Zn}V_{Zn})^{-}$  complex, acting as a deep compensating acceptor, is responsible for the suppressed net carrier concentration in highly Al-doped ZnO samples. Similar conclusions hold also for highly Ga-doped samples, where positron annihilation spectroscopy (PAS) studies revealed a concentration of point defects involving  $V_{Zn}$  in excess of  $10^{19} \text{ cm}^{-3}$  (this lower limit is due to saturation of the PAS signal).<sup>8</sup> On the basis of these arguments and to summarize, the reverse reaction in Eq. (1) is expected to be strongly suppressed in heavily Ga/Al-doped polycrystalline ZnO films, yielding a high steady-state concentration of  $(Ga_{Zn}V_{Zn})^{-}$  [or  $(Al_{Zn}V_{Zn})^{-}$ ] complexes.

#### B. Influence of the Fermi-level position

The abrupt front observed for all the diffusion profiles (Fig. 1) indicates that the Ga dopants induce a spatial variation of the charge carrier concentration (i.e., a Fermi level dependence). The high concentration of Ga donor dopants in the indiffused region ( $4 \times 10^{19} - 1 \times 10^{20} \text{ cm}^{-3}$ ) is about 6 orders of magnitude higher than the net charge carrier concentration in the bulk ( $2 \times 10^{13} \text{ cm}^{-3}$ ), where the latter is deduced from the measured resistivity of the as-received samples and assuming a bulk electron mobility of  $100 \text{ cm}^2/\text{V s}$ .

The double acceptor level of  $V_{Zn}$  is located in the lower part of the band gap,<sup>16</sup> and the double negative charge state is the prevailing one in n-type samples. The local concentration of  $V_{Zn}^{-2}$ , mediating the Ga diffusion in the ZnO bulk [cf. Eq. (1)], can be expressed via the local Fermi level position ( $\epsilon_F$ ) by

$$[V_{Zn}^{-2}] = N_{Zn} e^{-\frac{E_{f,0}(V_{Zn}^{-2}) - 2\epsilon_F}{k_B T}}, \quad (2)$$

where  $N_{Zn}$  is the total number of Zn sites per unit volume,  $E_{f,0}(V_{Zn}^{-2})$  is the formation energy of  $V_{Zn}^{-2}$  at the valence band edge (i.e., when  $\epsilon_F = 0$ ),  $k_B$  is the Boltzmann constant, and  $T$  is the absolute temperature. This means that the formation of  $V_{Zn}^{-2}$  is regarded as an instantaneous process with a local

equilibrium concentration governed by Eq. (2). Hence,  $\epsilon_F$  has a decisive impact on the RD-modelling results. For the simulated curves, a fixed value of  $E_{f,0}(V_{Zn}^{-2}) = 7.4$  eV is used, resulting in an adequate fit with the experimental data. This is also in reasonable agreement with previous DFT-predictions of  $E_{f,0}(V_{Zn}^{-2})$  under O-rich conditions.<sup>14,17</sup> Moreover, a binding energy  $E_b(\text{Ga}_{Zn}V_{Zn})^- = 1.25$  eV for the complex, as previously predicted by DFT-calculations,<sup>6</sup> is used as a fixed parameter in the RD-simulations.

### C. Comparison between experimental and RD modelling results

Figure 2 shows the RD model fitted to the experimental isochronal diffusion profiles. The diffusion simulations adequately reproduce the experimental diffusion profiles and an activation energy of  $E_{a,\text{complex}} = 2.3 \pm 0.1$  eV with a pre-exponential factor of  $D_0 = 8_{-5}^{+15} \times 10^{-2} \text{ cm}^2 \text{ s}^{-1}$  is extracted for the diffusion of  $\text{Ga}_{Zn}V_{Zn}$  (Fig. 3). In the simulations (Fig. 2), the error of the fitted diffusivity values is comparable to the marker size ( $\sim 3\%$ ), as determined by monitoring the agreement between the experimental and the fitted profiles when varying the diffusivity parameter.

Since the extracted  $E_{a,\text{complex}}$ -value represents the activation energy for diffusion of an already formed complex, i.e., the migration energy  $E_m = E_{a,\text{complex}} = 2.3$  eV, it enables a direct comparison with theoretical estimates. Here, it must be noted that the obtained migration energy  $E_m$  for  $\text{Ga}_{Zn}V_{Zn}$  is not unique as it depends on the presumed values of  $E_{f,0}(V_{Zn}^{-2})$  and  $E_b(\text{Ga}_{Zn}V_{Zn})^-$  in the RD-simulations. However, using the DFT value of  $E_b(\text{Ga}_{Zn}V_{Zn})^- = 1.25$  eV reported by Steiauf *et al.*,<sup>6</sup> our results are in excellent agreement with their theoretically predicted migration barrier of 2.23 eV (Ref. 6) for  $\text{Ga}_{Zn}V_{Zn}$ .

Figure 3 shows the present diffusivity values together with previously reported experimental data by Norman<sup>4</sup> and

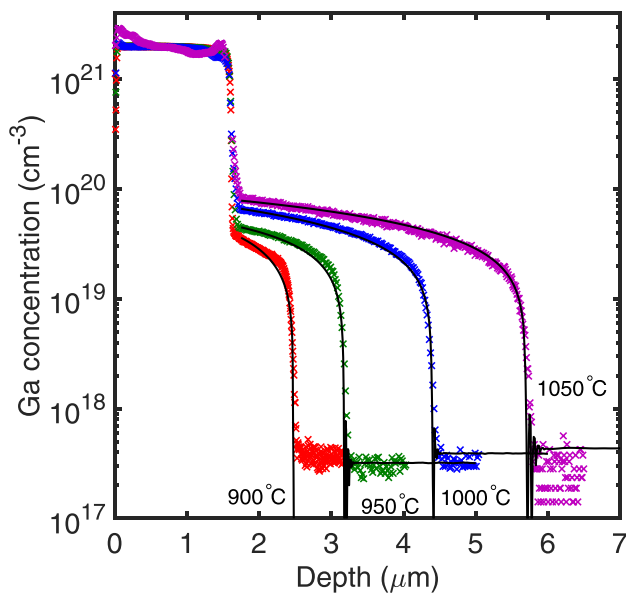


FIG. 2. RD model (solid lines) fitted to the experimental isochronal Ga diffusion profiles of the sample heat treated sequentially for 30 min from 900 °C to 1050 °C. The numerical accuracy of the fitted diffusivity values is better than 3%.

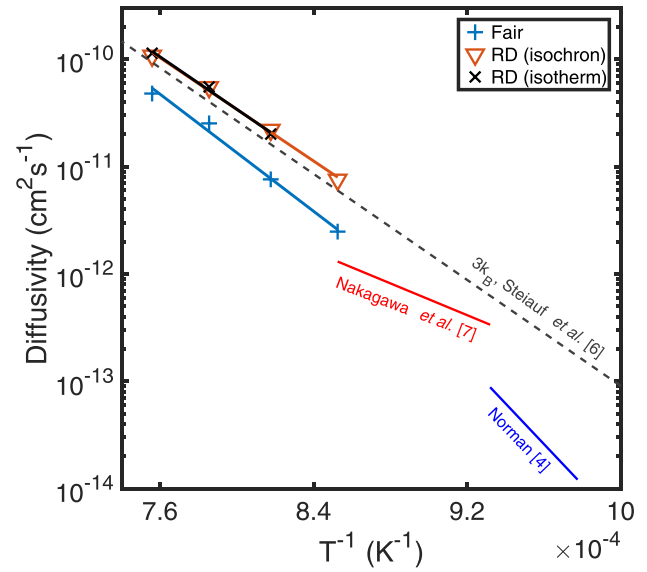


FIG. 3. Diffusivities of Ga and  $\text{Ga}_{Zn}V_{Zn}$  (RD) in ZnO. For the calculated values from Steiauf *et al.*,<sup>6</sup> ( $E_a^{\text{Steiauf}} = 2.45$  eV), the entropy contribution is set to  $3k_B$ , corresponding to a prefactor of  $2 \times 10^{-1} \text{ cm}^2 \text{ s}^{-1}$ .

Nakagawa *et al.*<sup>7</sup> Theoretical data from first-principles calculations for the total activation energy<sup>6</sup> are also included for comparison. Note that  $D_0$  is merely a structural entity,<sup>18</sup>  $D_0^{\text{ZnO}[0001]} = (3/4)fc^2\Gamma_0e^{S/k_B}$ , where  $f \leq 1$  is a correlation factor,  $c$  is the jump distance equal to  $3.25 \text{ \AA}$  in ZnO,  $\Gamma_0 \approx 10^{13} \text{ s}^{-1}$  being the typical phonon frequency, and  $S$  is the entropy contribution. For  $S=0$  and  $f=1$ , this results in  $D_0 \approx 10^{-2} \text{ cm}^2 \text{ s}^{-1}$ , which is rather close to the value extracted from the RD modeling and suggests a jump process with a small entropy effect. The obtained diffusion parameters are listed in Table I, together with previously reported values by other authors. A solubility of the  $\text{Ga}_{Zn}V_{Zn}$  complex is found to be  $S_{\text{Ga}_{Zn}V_{Zn}} = 1 \times 10^{23} \exp(-1.1 \text{ eV}/k_B T) \text{ cm}^{-3}$ , which is about one order of magnitude lower than the measured chemical concentration of Ga.

Further, isothermal diffusion experiments were performed in order to reveal any transient processes. Figure 4 shows the experimental isothermal Ga diffusion profiles of three samples heat treated at 950, 1000, or 1050 °C, respectively, for durations in the range of 20 min to 5 h. Simulation

TABLE I. Extracted diffusion parameters for Ga in ZnO, together with previous theoretical and experimental results. With  $D_0$  being the pre-exponential factor,  $E_m$  is the migration barrier for the exchange process of  $\text{Ga}_{Zn}V_{Zn}$  and  $E_a$  is the total activation energy for diffusion.

	$D_0$ (cm <sup>2</sup> /s)	$E_m$ (eV)	$E_a$ (eV)
Fair	1	...	$2.7 \pm 0.1$
RD (isochron)	$8 \times 10^{-2}$	$2.3 \pm 0.1$	$3.0^d \pm 0.2$
Theo <sup>a</sup>	...	2.23	2.45
Exp <sup>b</sup>	$2.7 \times 10^{-6}$	...	1.47
Exp <sup>c</sup>	$3.6 \times 10^4$	...	3.75

<sup>a</sup>Steiauf *et al.*<sup>6</sup>

<sup>b</sup>Nakagawa *et al.*<sup>7</sup>

<sup>c</sup>Norman.<sup>4</sup>

<sup>d</sup>Obtained from Eq. (5).

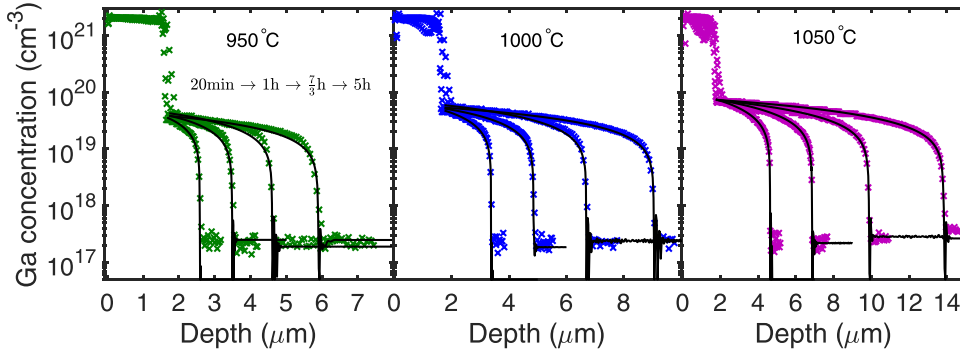


FIG. 4. Isothermal Ga diffusion profiles of the three samples heat treated sequentially for durations in the range of 20 min to 5 h at 950 °C, 1000 °C, or 1050 °C. The solid lines are the simulation results from our RD modeling. The numerical accuracy of the fitted diffusivity values is better than 3%.

results obtained from the RD model are also included in Fig. 4, and they follow closely the experimental data. A square-root of time dependence holds for the isothermal diffusion profiles, which supports the assumption that local equilibrium of the reaction in Eq. (1) is rapidly established. A migration barrier of  $E_m = 2.3$  eV with a pre-exponential factor of  $1 \times 10^{-1} \text{ cm}^2 \text{ s}^{-1}$  is obtained from the isothermal data, substantiating the validity of the results deduced from the isochronal experiment in Fig. 2. The corresponding diffusivities, where each value is taken as the mean of the set of measurements at different times, are displayed in Fig. 3. In this regard, we note that the slightly abnormal shape of the 900 °C isochronal experiment (Figs. 1 and 2) may be due to initial transient effects at this low temperature before steady state is fully established. However, based on the consistent trend of the Arrhenius behavior of the extracted diffusivities (Fig. 3), we consider the 900 °C experiment to primarily reflect a similar diffusion behavior as that at the higher temperatures.

In addition to provide a value for the  $\text{Ga}_{\text{Zn}}\text{V}_{\text{Zn}}$  migration barrier, the RD model has also been applied to estimate the total activation energy for the Ga diffusion,  $E_a$ . As schematically illustrated in Fig. 5, to move  $\text{Ga}_{\text{Zn}}$  via  $\text{V}_{\text{Zn}}$ , it requires the formation and presence of a  $\text{V}_{\text{Zn}}$  as a next-nearest neighbour. That is,  $\text{V}_{\text{Zn}}$  must form at some site and subsequently approach the  $\text{Ga}_{\text{Zn}}$ . The associated  $\text{V}_{\text{Zn}}$  must then either (i) exchange with  $\text{Ga}_{\text{Zn}}$  and dissociate or (ii) exchange and rotate around the  $\text{Ga}_{\text{Zn}}$ . In a first approximation, the total activation energy for the diffusion of Ga can be expressed as a sum of all the above processes

$$E_a = E_f(\text{V}_{\text{Zn}}^{-2}) + E_m(\text{V}_{\text{Zn}}^{-2}) + E_m(\text{Ga}_{\text{Zn}}\text{V}_{\text{Zn}})^- - E_d(\text{Ga}_{\text{Zn}}\text{V}_{\text{Zn}})^-, \quad (3)$$

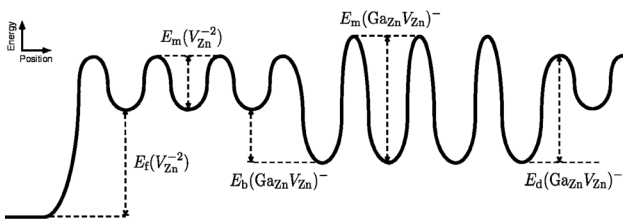


FIG. 5. Energy diagram illustrating the involved processes for the diffusion of Ga. From left: the formation of  $\text{V}_{\text{Zn}}^{-2}$ , the migration of  $\text{V}_{\text{Zn}}^{-2}$ , the binding of  $\text{V}_{\text{Zn}}^{-2}$  with  $\text{Ga}_{\text{Zn}}^+$ , the migration of  $(\text{Ga}_{\text{Zn}}\text{V}_{\text{Zn}})^-$ , and the dissociation of the complex.

where  $E_f(\text{V}_{\text{Zn}}^{-2})$  is the formation energy of  $\text{V}_{\text{Zn}}^{-2}$ ,  $E_m(\text{V}_{\text{Zn}}^{-2})$  and  $E_m(\text{Ga}_{\text{Zn}}\text{V}_{\text{Zn}})^-$  are the migration barrier for  $\text{V}_{\text{Zn}}^{-2}$  and the barrier for the migration of  $(\text{Ga}_{\text{Zn}}\text{V}_{\text{Zn}})^-$ , respectively, while  $E_d(\text{Ga}_{\text{Zn}}\text{V}_{\text{Zn}})^-$  is the energy required to dissociate the complex. The dissociation barrier can in turn be approximated as

$$E_d(\text{Ga}_{\text{Zn}}\text{V}_{\text{Zn}})^- = E_b(\text{Ga}_{\text{Zn}}\text{V}_{\text{Zn}})^- + E_m(\text{V}_{\text{Zn}}^{-2}) - k_B T, \quad (4)$$

where  $E_b(\text{Ga}_{\text{Zn}}\text{V}_{\text{Zn}})^-$  is the binding energy of the complex. In the modeling, we use an effective capture radius of  $R_c = 1$  nm for the trapping of  $\text{V}_{\text{Zn}}^{-2}$  by  $\text{Ga}_{\text{Zn}}^+$ , leading to the inclusion of  $k_B T$  in Eq. (4). This term arises due to the slightly reduced (by the amount of  $k_B T$ ) potential energy of the dissociated  $\text{V}_{\text{Zn}}^{-2}$  at a distance  $R_c$  from  $\text{Ga}^+$  (see Ref. 19 for a general formalism). Inserting Eq. (4) into Eq. (3) gives

$$E_a = E_f(\text{V}_{\text{Zn}}^{-2}) - E_b(\text{Ga}_{\text{Zn}}\text{V}_{\text{Zn}})^- + E_m(\text{Ga}_{\text{Zn}}\text{V}_{\text{Zn}})^- + k_B T. \quad (5)$$

Here,  $E_f(\text{V}_{\text{Zn}}^{-2})$  is extracted from  $E_{f,0}(\text{V}_{\text{Zn}}^{-2})$  and the Fermi level position at the interface between the diffusion source and the bulk crystal ( $E_f(\text{V}_{\text{Zn}}^{-2}) = E_{f,0}(\text{V}_{\text{Zn}}^{-2}) - 2\epsilon_F$ ) is found to be 1.85 eV. With  $k_B T = 0.1$  eV, we obtain a total activation energy of  $E_a = 3.0$  eV for the diffusion of Ga in ZnO. Interestingly, the difference in  $E_a$  between our data and the theoretical ones in Ref. 6 can be attributed to a difference in  $E_{f,0}(\text{V}_{\text{Zn}}^{-2})$  used in the calculations of  $E_f(\text{V}_{\text{Zn}}^{-2})$ . Furthermore, we obtain an upper limit for  $E_d(\text{Ga}_{\text{Zn}}\text{V}_{\text{Zn}})^-$  of 3.05 eV, whereupon the model begins to deviate from the experimental data. Hence, in accord with Eq. (4),  $E_m(\text{V}_{\text{Zn}}^{-2})$  cannot exceed  $3.05 - 1.25 + 0.1 = 1.9$  eV and  $E_m(\text{Ga}_{\text{Zn}}\text{V}_{\text{Zn}})^-$  is the limiting migration barrier for the diffusion of Ga at these conditions (as schematically illustrated in Fig. 5). This conclusion is also fully supported by the quadratic Ga-concentration dependence of the Ga diffusivity, in accordance with several general and comprehensive studies of the concentration dependence of dopant diffusion in semiconductors.<sup>11–13</sup> In particular, it becomes evident that  $\text{V}_{\text{Zn}}^{-2}$  cannot be the defect controlling/limiting the migration process as this results in Ga diffusion profiles of very different shape than the experimental ones.<sup>11</sup>

#### D. Comparison between experimental and Fair modelling results

In order to further substantiate the results obtained from our RD model, we also analyse the experimental data using

another and more common approach to model dopant diffusion in semiconductors. The approach assumes each dopant to be in its isolated configuration, which is a valid approximation given that only a small fraction of the dopants exist in defect complexes. If one further accounts for the electric field arising from the non-uniform dopant distribution, giving rise to energy band bending, the dopant diffusion is described as a sum of the different charge state contributions.<sup>20</sup> In other words, the effective diffusion coefficient can be regarded as concentration dependent.<sup>11</sup> This is often denoted as the Fair model.<sup>21</sup> Considering only a double negatively charged defect  $X$  mediating the diffusion, the effective Ga diffusivity becomes

$$D_{\text{Ga}} = H D_{\text{Ga}^+X^{-2}}^i \left( \frac{n}{n_i} \right)^2. \quad (6)$$

In Eq. (6),  $H$  is a correction factor arising from the spatially varying Fermi level, taking values between 1 (intrinsic regime) and 2 (far-extrinsic regime). The superscript  $i$  denotes intrinsic conditions.  $n$  is the free carrier concentration, and  $n_i = \sqrt{N_C N_V} \exp\left(-\frac{E_g}{2k_B T}\right)$  is the intrinsic carrier concentration with  $N_C$  and  $N_V$  being the effective density of states at the conduction- and valence band edge, respectively. The  $(n/n_i)^2$  term is proportional to the number of double negatively charged defects and reflects the probability-of-existence of, e.g.,  $V_{\text{Zn}}^{-2}$ . The ZnO band gap  $E_g$  equals 3.4 eV at room temperature but is significantly reduced at the diffusion temperatures employed. We have used data from band gap measurements of ZnO in the temperature range of 100–500 °C by Hauschild *et al.*<sup>22</sup> and then assumed a similar linear dependence at higher temperatures:  $\Delta E_g(T) = 80.5 - 0.52T$  (meV).

As can be seen in Fig. 6, Fair's model [Eq. (6)] adequately reproduces the experimental data recorded after

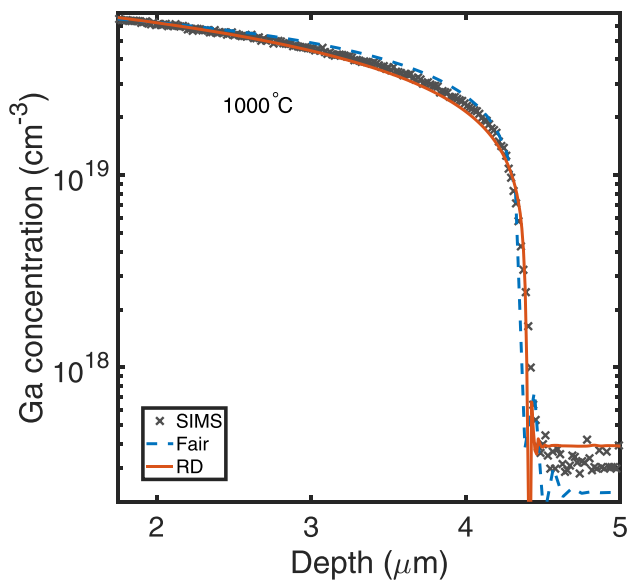


FIG. 6. Comparison of the Fair model and the reaction diffusion (RD) model, as fitted to the experimentally obtained SIMS profile after the 1000 °C (isochronal) treatment. Note that the data from the deposited film have been excluded for clarity.

30 min at 1000 °C (isochronal annealing) but gives a slightly higher concentration close to the diffusion tail as compared to that of the RD model. An activation energy of  $E_a = 2.7$  eV with a pre-exponential factor of  $D_0 = 1 \text{ cm}^2 \text{ s}^{-1}$  is obtained for  $D_{\text{Ga}}$  (see Fig. 3), where complete ionization of  $\text{Ga}_{\text{Zn}}$  is assumed (i.e.,  $n$  is taken to be given by the solid solubility of Ga,  $n = S_{\text{Ga}} = 7 \times 10^{22} \exp(-0.8 \text{ eV}/k_B T) \text{ cm}^{-3}$ ).  $D_{\text{Ga}}$  extracted from Eq. (6) is an effective (or apparent) diffusion coefficient given by the product of the equilibrium concentration and the diffusivity of  $(\text{Ga}_{\text{Zn}}V_{\text{Zn}})^{-}$  divided by the concentration of  $\text{Ga}_{\text{Zn}}^+$ .<sup>11,20</sup> Hence, the  $E_a$  value of 2.7 eV does not only contain the activation energy for migration of  $(\text{Ga}_{\text{Zn}}V_{\text{Zn}})^{-}$  but also the difference between the formation energies of  $(\text{Ga}_{\text{Zn}}V_{\text{Zn}})^{-}$  and  $\text{Ga}_{\text{Zn}}^+$ . Thus, a direct comparison with the results from the RD-modeling and  $E_m(\text{Ga}_{\text{Zn}}V_{\text{Zn}})^{-}$  is not valid. However, if  $E_m(\text{Ga}_{\text{Zn}}V_{\text{Zn}})^{-}$  is assumed to be 2.3 eV, as extracted from the RD-modeling and in close agreement with the DFT prediction by Steiauf *et al.*,<sup>6</sup> one obtains  $E_f(\text{Ga}_{\text{Zn}}V_{\text{Zn}})^{-} - E_f(\text{Ga}_{\text{Zn}}^+) \approx 0.4$  eV at the temperatures of diffusion. Indeed, such a relatively small difference between  $E_f(\text{Ga}_{\text{Zn}}V_{\text{Zn}})^{-}$  and  $E_f(\text{Ga}_{\text{Zn}}^+)$  is fully consistent with the DFT results by Demchenko *et al.*<sup>14</sup> under O-rich conditions, accounting for the  $E_g$  narrowing with temperature and that extrinsic conditions still prevail in the highly Ga-doped ZnO films during diffusion, i.e.,  $\epsilon_F$  remains close to the conduction band edge. Moreover and despite some uncertainty, it is interesting to note that the total (or effective) value of  $3.0 \pm 0.2$  eV for the Ga diffusion extracted from the RD-modeling [Eq. (5) and Table I] is in fair/reasonable agreement with the effective value of  $2.7 \pm 0.1$  eV from the Fair modeling. The discrepancy between the two values (3.0 versus 2.7 eV) is essentially within the accuracy of data analysis of the two approaches, especially considering the limited accuracy of DFT estimates and the high concentration of  $(\text{Ga}_{\text{Zn}}V_{\text{Zn}})^{-}$  complexes. The latter may also partly violate the implicit assumption regarding a much lower concentration of  $(\text{Ga}_{\text{Zn}}V_{\text{Zn}})^{-}$  complexes than that of  $\text{Ga}_{\text{Zn}}^+$  donors made in the Fair modeling.

As previously discussed, the donor dopant concentration is about 6 orders of magnitude higher in the indiffused region compared to that of the bulk. In addition, as demonstrated in Fig. 6 by the comparison between the RD-type model [Eq. (1)] and the Fair model [Eq. (6)], a quadratic dependence between the Ga diffusivity and the Ga concentration adequately explains the experimental Ga diffusion profile. Hence, the modelling results provide strong support for a  $V_{\text{Zn}}^{-2}$ -mediated diffusion of Ga with an exponential dependence on the Fermi-level position ( $\epsilon_F$ ). However, for an unambiguous conclusion on the diffusion mechanism and especially the  $\epsilon_F$  dependence, isoconcentration diffusion experiments with  $\epsilon_F$  pinned at given positions are desirable. Indeed, using undoped and *in situ* doped isotopic heterostructure ZnO samples, Azarov *et al.*<sup>23</sup> have recently shown experimentally that the Zn self-diffusion is enhanced by several orders of magnitude as  $\epsilon_F$  is shifted towards the conduction band edge. Accordingly,  $V_{\text{Zn}}^{-2}$  was regarded as the mediating defect of the Zn self-diffusion and an upper limit of 1.5 eV was determined for  $E_m(V_{\text{Zn}}^{-2})$ , fully consistent with our modelling results. Moreover, preliminary PAS and SIMS

data for Al-doped ZnO samples reveal a quadratic relation between the  $V_{\text{Zn}}$  and Al concentrations,<sup>24</sup> corroborating  $V_{\text{Zn}}^{-2}$  as a prime defect promoting Al diffusion. A similar result is also anticipated for Ga-doped ZnO samples and further studies on this subject are being pursued.

#### IV. SUMMARY

The diffusion of Ga in monocrystalline ZnO is found to be well described as vacancy mediated through the formation (and subsequent dissociation) of an intermediate dopant-vacancy complex. Both simulation results from our RD model and from Fair's model suggest that the diffusion of Ga proceeds by one single mechanism throughout the studied temperature interval, 900–1050 °C. From the RD-simulations, this mechanism is suggested to be driven by  $V_{\text{Zn}}^{-2}$  through the diffusion of  $(\text{Ga}_{\text{Zn}}V_{\text{Zn}})^{-}$ . Utilizing DFT estimates of  $E_f(V_{\text{Zn}}^{-2})$  and  $E_b(\text{Ga}_{\text{Zn}}V_{\text{Zn}})^{-}$ , a migration barrier of  $E_m = 2.3$  eV with a pre-exponential factor of  $8 \times 10^{-2} \text{ cm}^2 \text{ s}^{-1}$  is deduced for the  $(\text{Ga}_{\text{Zn}}V_{\text{Zn}})^{-}$  complex from the RD-modeling, in close agreement with results from recent first principles calculations.<sup>6</sup> The Fair modeling gives a total/effective energy of  $2.7 \pm 0.1$  eV for Ga diffusion in ZnO which is in reasonable agreement with the total/effective value of  $3.0 \pm 0.2$  eV obtained from the RD-modeling. Previous experimental values in the literature for the total/effective activation energy of Ga diffusion in ZnO scatter over a range of more than 2 eV (Refs. 4 and 7) and our value is approximately in the middle of this range.

#### ACKNOWLEDGMENTS

Financial support from the Research Council of Norway for funding of the DYNAZOX-project (Grant No. 221992), Salient (Grant No. 239895), the University of Oslo, and the Norwegian Micro- and Nano-Fabrication Facility (NorFab 245963) is gratefully acknowledged.

- <sup>1</sup>T. Minami, H. Sato, H. Nanto, and S. Takata, *Jpn. J. Appl. Phys., Part 2* **24**, L781 (1985), ISSN 1347-4065.
- <sup>2</sup>H. Y. Liu, V. Avrutin, N. Izyumskaya, M. A. Reshchikov, Ü. Özgür, and H. Morkoç, *Phys. Status Solidi RRL* **4**, 70 (2010), ISSN 1862-6270.
- <sup>3</sup>J. Nomoto, M. Konagai, K. Okada, T. Ito, T. Miyata, and T. Minami, *Thin Solid Films* **518**, 2937 (2010), ISSN 0040-6090.
- <sup>4</sup>V. Norman, *Aust. J. Chem.* **22**, 325 (1969).
- <sup>5</sup>K. M. Johansen, L. Vines, T. S. Bjørheim, R. Schifano, and B. G. Svensson, *Phys. Rev. Appl.* **3**, 024003 (2015).
- <sup>6</sup>D. Steiauf, J. L. Lyons, A. Janotti, and C. G. V. d. Walle, *APL Mater.* **2**, 096101 (2014), ISSN 2166-532X.
- <sup>7</sup>T. Nakagawa, I. Sakaguchi, M. Uematsu, Y. Sato, N. Ohashi, H. Haneda, and Y. Ikuhara, *Jpn. J. Appl. Phys., Part 1* **46**, 4099 (2007), ISSN 1347-4065.
- <sup>8</sup>D. C. Look, K. D. Leedy, L. Vines, B. G. Svensson, A. Zubiaga, F. Tuomisto, D. R. Douth, and L. J. Brillson, *Phys. Rev. B* **84**, 115202 (2011).
- <sup>9</sup>J. E. Stehr, K. M. Johansen, T. S. Bjørheim, L. Vines, B. G. Svensson, W. M. Chen, and I. A. Buyanova, *Phys. Rev. Appl.* **2**, 021001 (2014).
- <sup>10</sup>S. M. Hu, *Phys. Rev.* **180**, 773 (1969).
- <sup>11</sup>H. Bracht, *Phys. Rev. B* **75**, 035210 (2007).
- <sup>12</sup>M. Uematsu, *J. Appl. Phys.* **82**, 2228 (1997), ISSN 0021-8979, 1089-7550.
- <sup>13</sup>U. M. Gosele, *Annu. Rev. Mater. Sci.* **18**, 257 (1988).
- <sup>14</sup>D. O. Demchenko, B. Earles, H. Y. Liu, V. Avrutin, N. Izyumskaya, Ü. Özgür, and H. Morkoç, *Phys. Rev. B* **84**, 075201 (2011).
- <sup>15</sup>J. T-Thienprasert, S. Rujirawat, W. Klysubun, J. N. Duenow, T. J. Coutts, S. B. Zhang, D. C. Look, and S. Limpijumnong, *Phys. Rev. Lett.* **110**, 055502 (2013).
- <sup>16</sup>A. Janotti and C. G. Van de Walle, *Phys. Rev. B* **76**, 165202 (2007).
- <sup>17</sup>Y. K. Frodason, K. M. Johansen, T. S. Bjørheim, B. G. Svensson, and A. Alkauskas, *Phys. Rev. B* **95**, 094105 (2017).
- <sup>18</sup>J. Philibert, *Atom Movements – Diffusion and Mass Transport in Solids* (Les Editions De Physique, 1991).
- <sup>19</sup>M. Janson, Ph.D. thesis, KTH, Royal Institute of Technology, 2003.
- <sup>20</sup>P. M. Fahey, P. B. Griffin, and J. D. Plummer, *Rev. Mod. Phys.* **61**, 289 (1989).
- <sup>21</sup>R. B. Fair and J. C. C. Tsai, *J. Electrochem. Soc.* **124**, 1107 (1977), ISSN 0013-4651, 1945-7111.
- <sup>22</sup>R. Hauschild, H. Priller, M. Decker, J. Brückner, H. Kalt, and C. Klingshim, *Phys. Status Solidi C* **3**, 976 (2006), ISSN 1610-1642.
- <sup>23</sup>A. Azarov, V. Venkatachalapathy, Z. Mei, L. Liu, X. Du, A. Galeckas, E. Monakhov, B. G. Svensson, and A. Kuznetsov, *Phys. Rev. B* **94**, 195208 (2016).
- <sup>24</sup>T. N. Sky, K. M. Johansen, F. Tuomisto, B. G. Svensson, and L. Vines, "Influence of Fermi-level position on vacancy-assisted diffusion of aluminum in zinc oxide" (unpublished).